“Wave-Turbulence Interactions in the Oceans”

https://oceanturbulence.github.io

Patrice Klein (Caltech/JPL/Ifremer)

(XV) Interactions between waves and balanced motions

Propagation of waves in an inhomogeneous medium:

Young and Ben-Jelloul approach

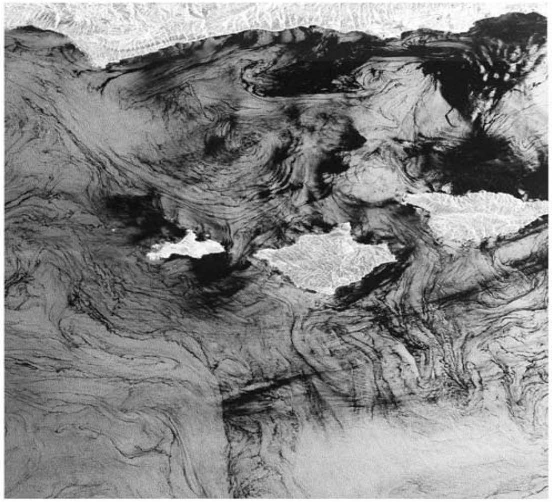

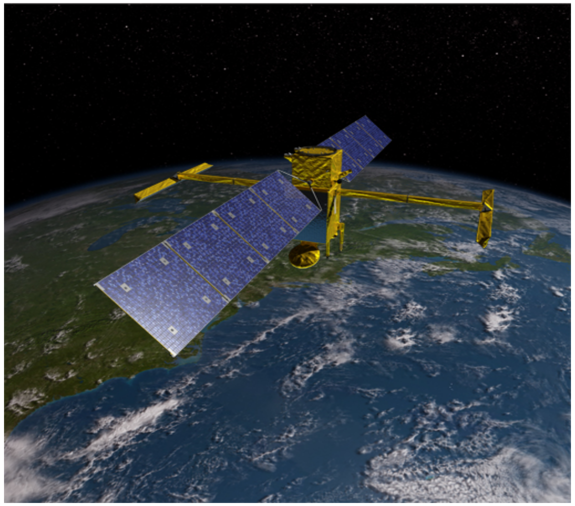


4 Oct 2012 00:00
4 Oct 2012 00:00
4 Oct 2012 00:00
4 Oct 2012 00:00
4 Oct 2012 00:00
4 Oct 2012 00:00
4 Oct 2012 00:00
4 Oct 2012 00:00
4 Oct 2012 00:00
4 Oct 2012 00:00
4 Oct 2012 00:00
4 Oct 2012 00:00
3 Oct 2012 00:00
4 Oct 2012 00:00
3 Oct 2012 00:00
3 Oct 2012 00:00
4 Oct 2012 00:00
4 Oct 2012 00:00
4 Oct 2012 00:00
4 Oct 2012 00:00
4 Oct 2012 00:00
3 Oct 2012 00:00
3 Oct 2012 00:00
4 Oct 2012 00:00
3 Oct 2012 00:00
3 Oct 2012 00:00
4 Oct 2012 00:00
4 Oct 2012 00:00
4 Oct 2012 00:00
4 Oct 2012 00:00
3 Oct 2012 00:00
3 Oct 2012 00:00
3 Oct 2012 00:00
3 Oct 2012 00:00
3 Oct 2012 00:00
3 Oct 2012 00:00
3 Oct 2012 00:00
3 Oct 2012 00:00
3 Oct 2012 00:00
3 Oct 2012 00:00
3 Oct 2012 00:00
3 Oct 2012 00:00
3 Oct 2012 00:00
3 Oct 2012 00:00
3 Oct 2012 00:00
3 Oct 2012 00:00
3 Oct 2012 00:00
3 Oct 2012 00:00
3 Oct 2012 00:00
3 Oct 2012 00:00
3 Oct 2012 00:00
3 Oct 2012 00:00
3 Oct 2012 00:00
3 Oct 2012 00:00
3 Oct 2012 00:00
3 Oct 2012 00:00
3 Oct 2012 00:00
3 Oct 2012 00:00
3 Oct 2012 00:00
3 Oct 2012 00:00
3 Oct 2012 00:00
3 Oct 2012 00:00
3 Oct 2012 00:00
3 Oct 2012 00:00

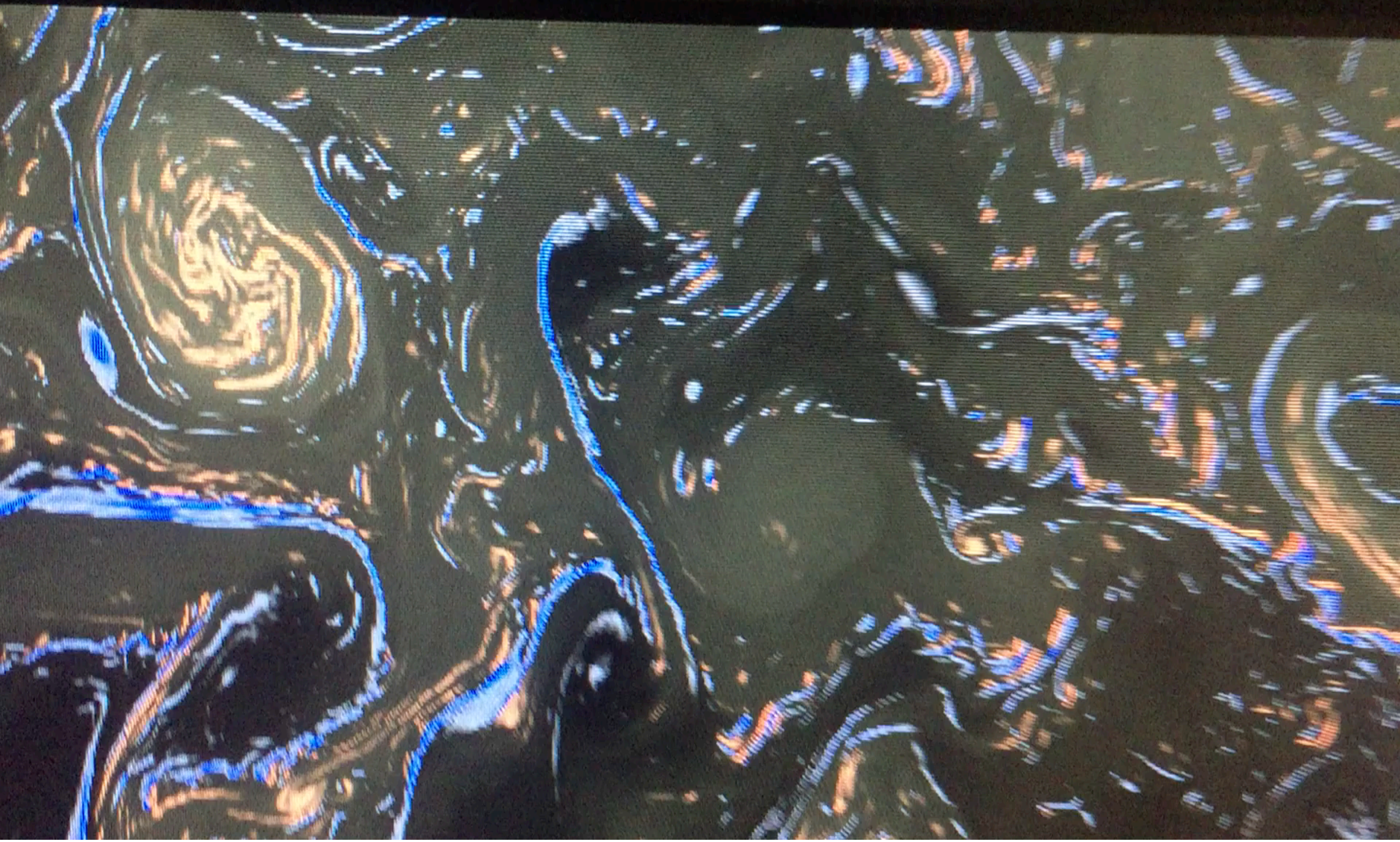

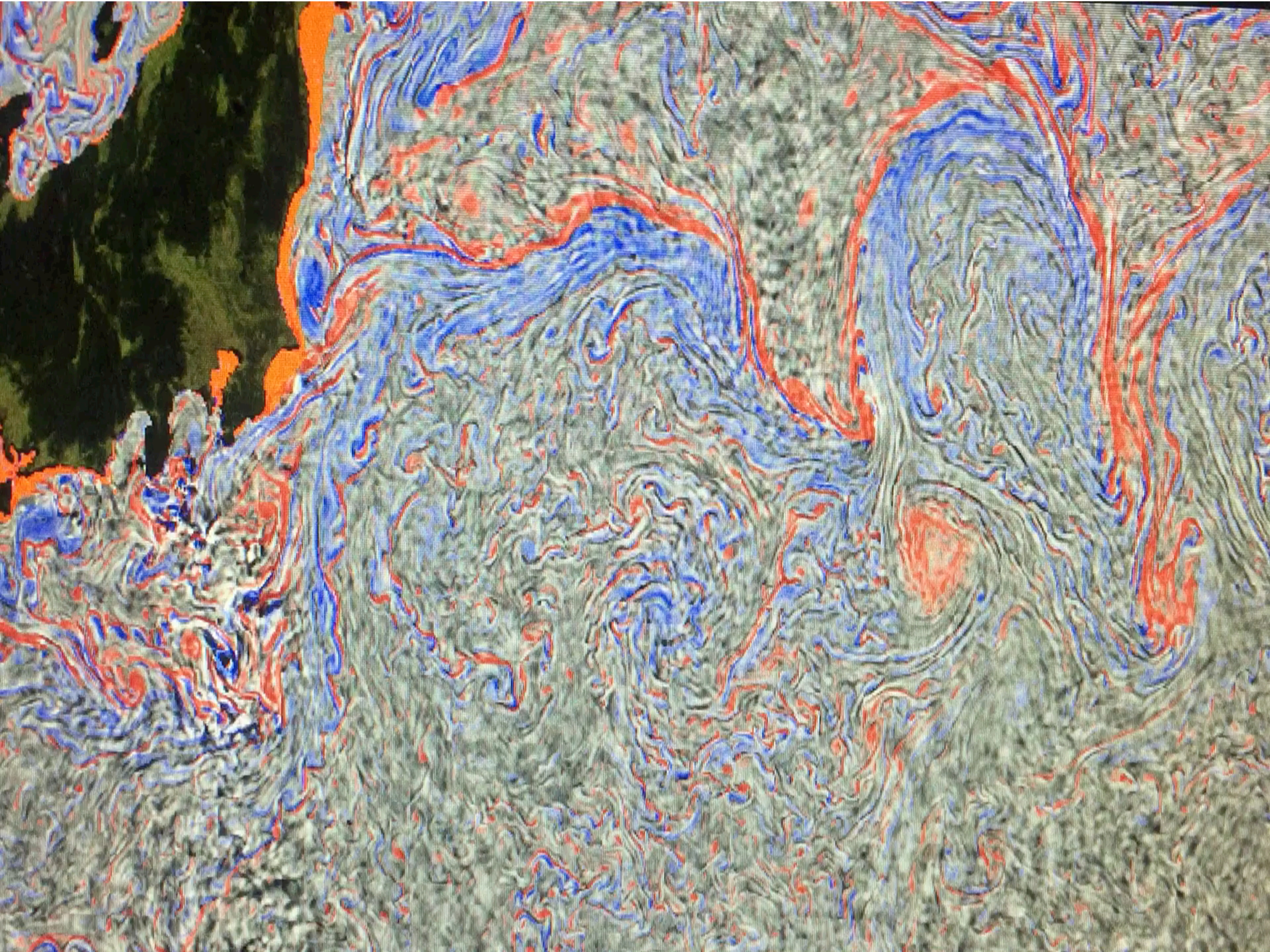

The <u>high frequency part of the wave spectrum</u> is characterized by <u>discrete bands!</u>

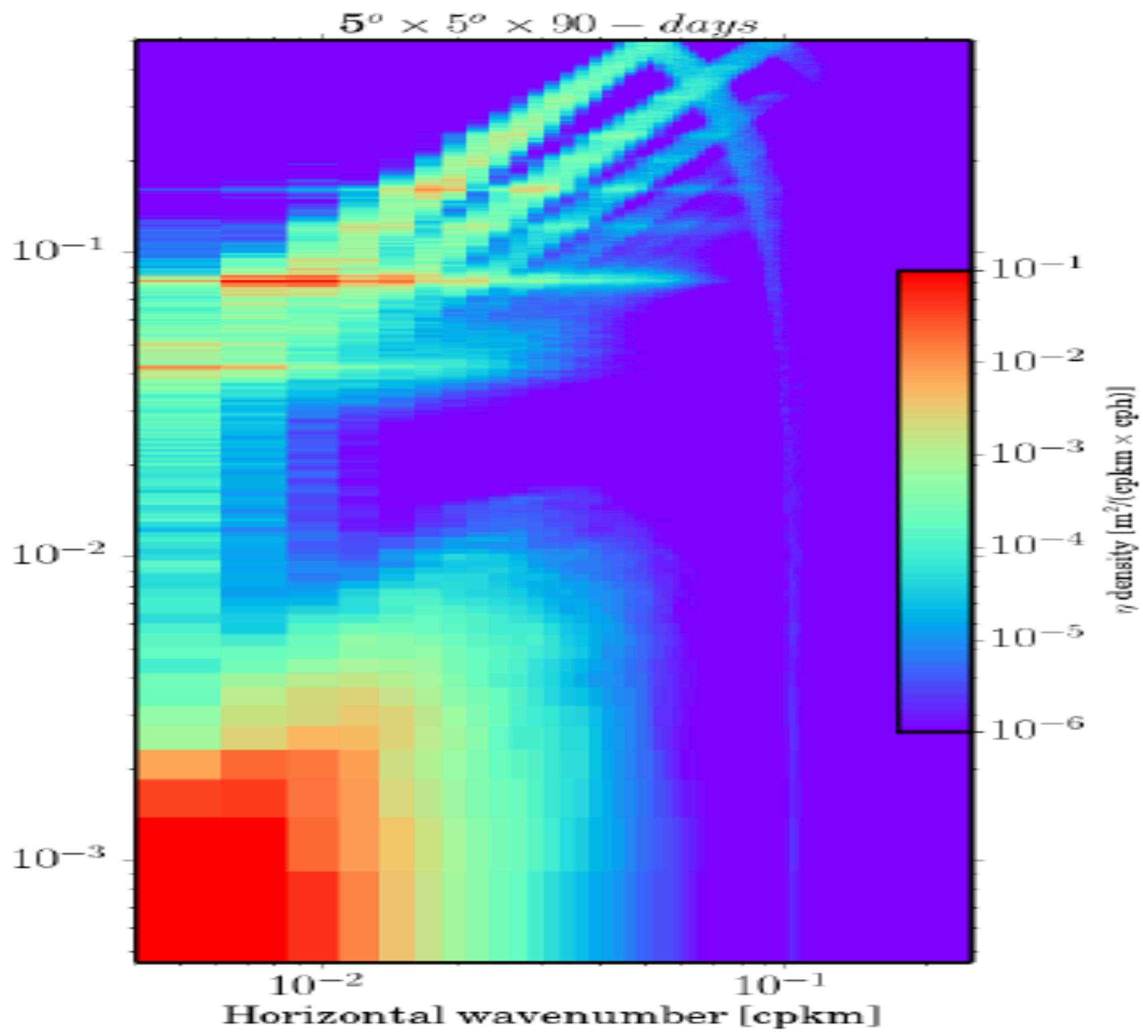

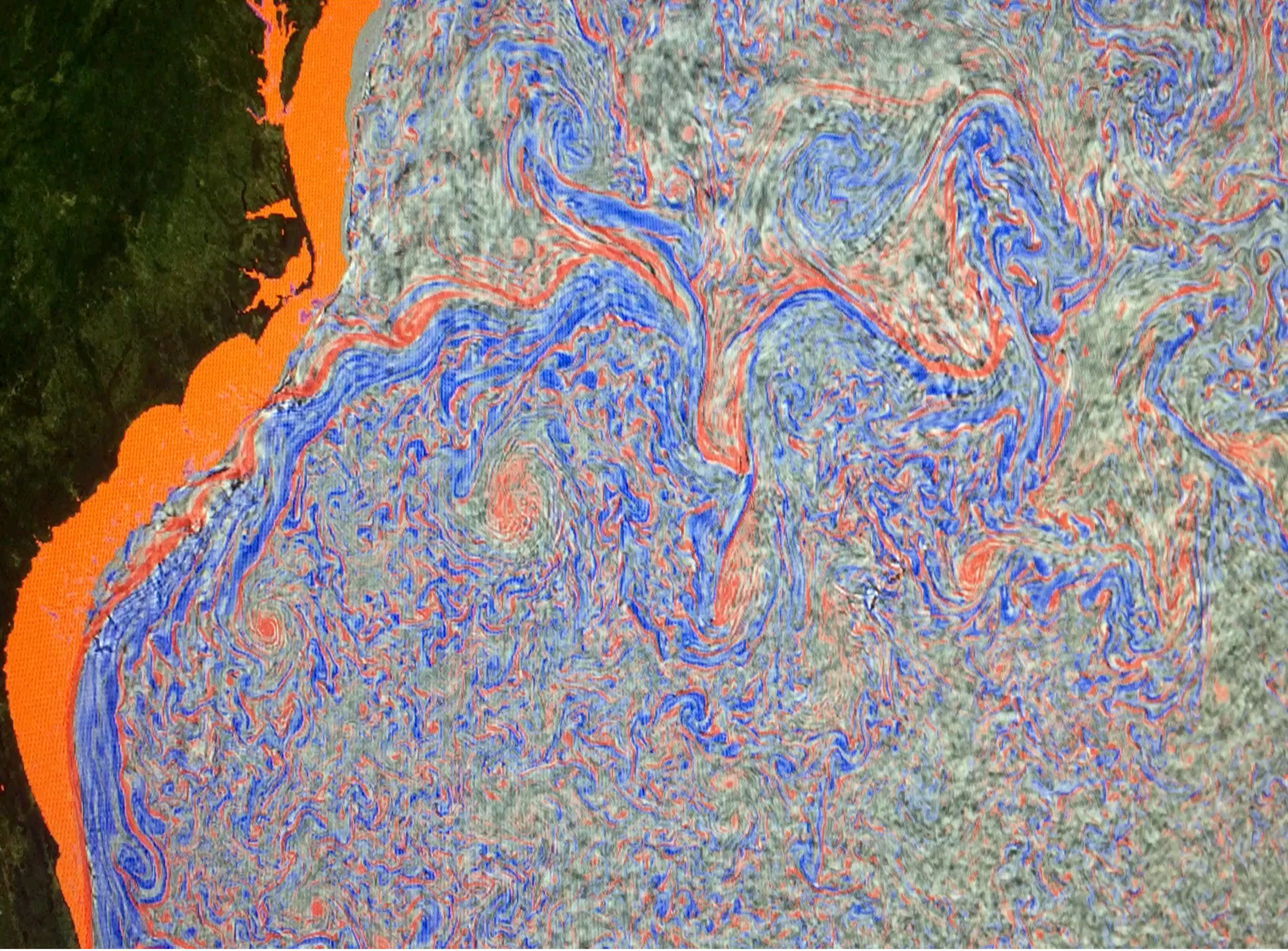

The high frequency part of the wave spectrum is characterized by discrete bands!

What mechanisms explain these characteristics?

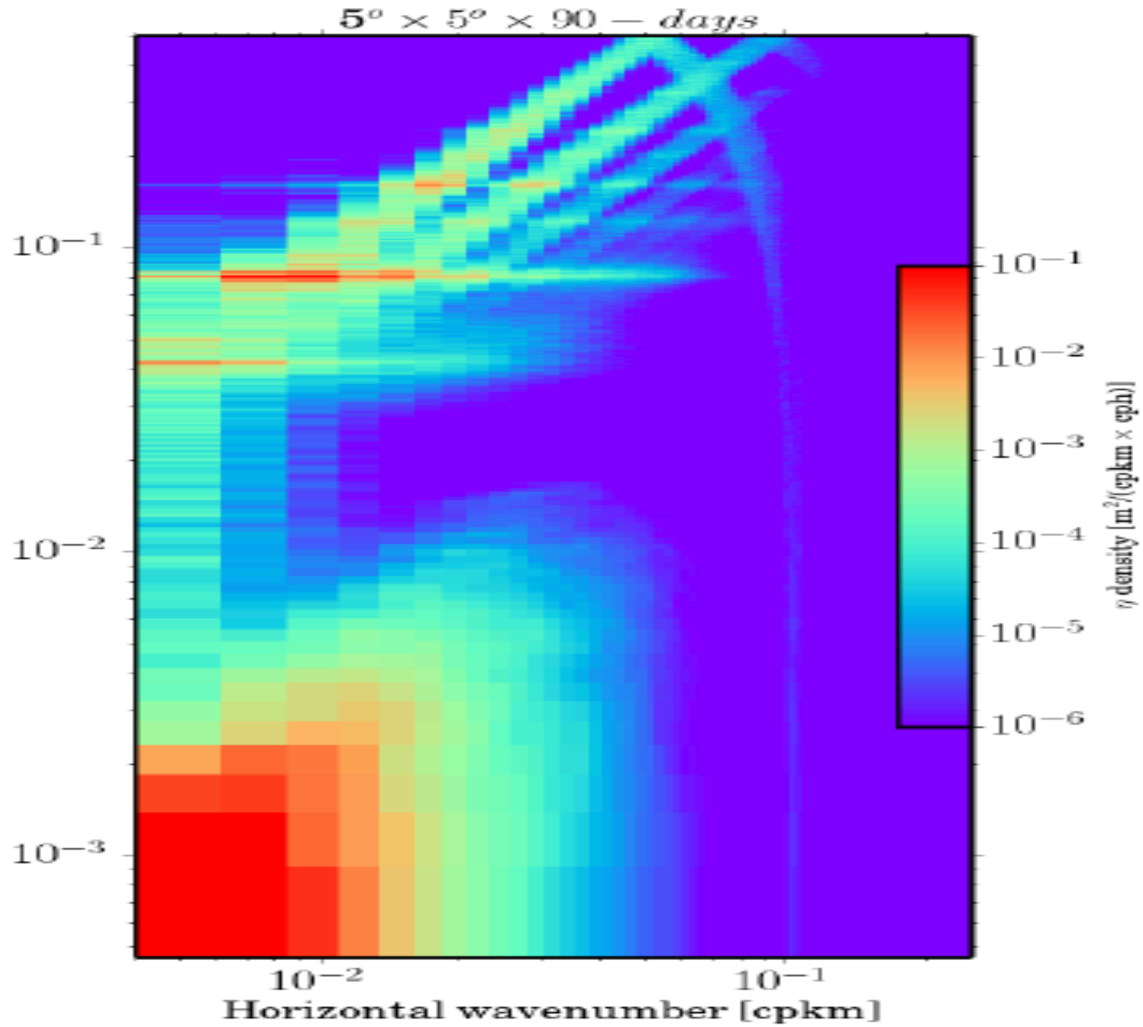

Wave propagation in a stationary barotropic jet: *V(x)*

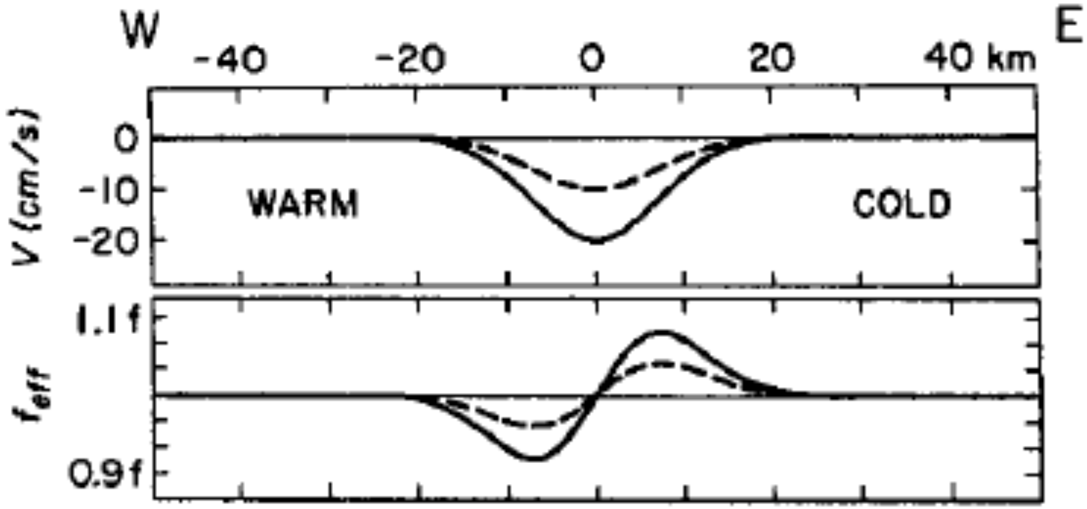

FIG. 4. A model southward baroclinic jet (upper frame) analogous to the North Pacific Subtropical Front, and the associated effective Coriolis frequency $f_{eff} = f + \zeta/2$ (lower frame). The solid curves represent values at the surface, and dashed curves values at a depth of 100 m. Internal waves propagate freely only for frequencies lying above the f_{eff}-curve.

$$\partial V/\partial x = 0.1f/10km$$

Kunze JPO 1985

$$p(x,y,z,t) = \sum_m p_m(x,y).F_m(z)$$

When N^2 is constant, $F_m(z) = cos(m.z)$ and $r_m^2 = \frac{N^2}{f^2.m^2}$

For baroclinic mode m:

$$\frac{\partial u}{\partial t} - (\mathrm{f}+\zeta)v = 0$$
$$\frac{\partial v}{\partial t} + \mathrm{f}u = -g'\frac{\partial h}{\partial y}$$
$$\frac{\partial h}{\partial t} + H_o\frac{\partial v}{\partial y} = 0$$

$$\boxed{\Rightarrow \frac{\partial^2 v}{\partial t^2} + f(f+\zeta)v - g'H_o\frac{\partial^2 v}{\partial y^2} = 0}$$

It was assumed that:

- the geostrophic jet is smoothly varying in space. The wave scales are smaller than the jet scale. => WKB approximation can be used.
- Wave-wave interactions are neglected.

Dispersion of internal gravity waves by a mesoscale eddy field
(characterized by a continuous wavenumber spectrum)

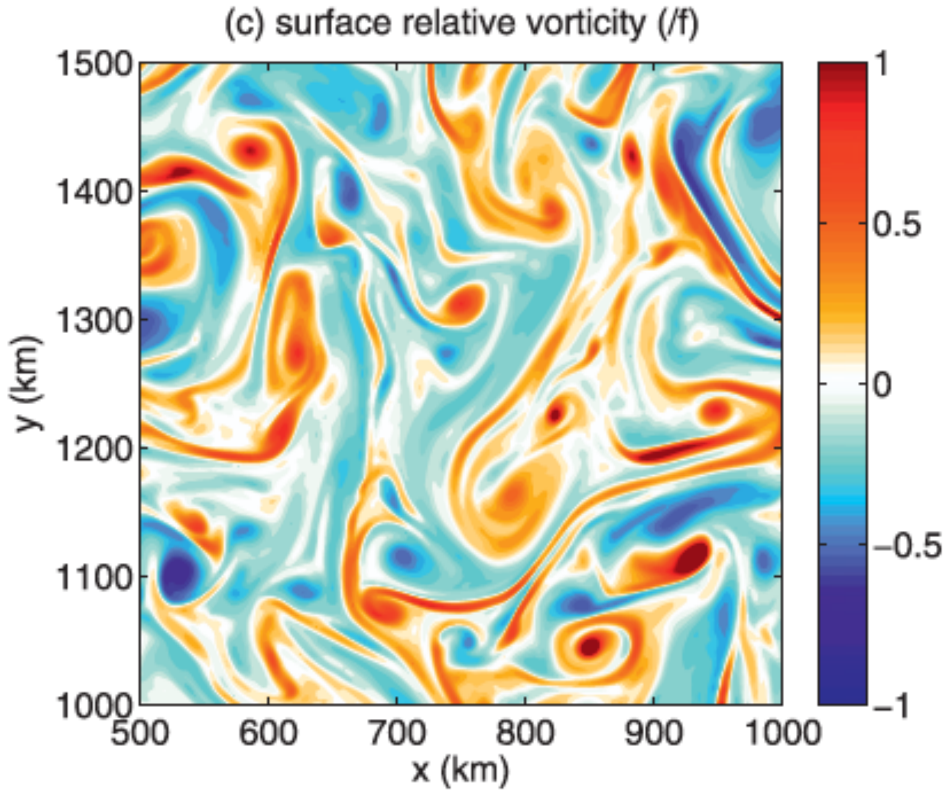

Assume now:

- **Wave scales can be close to the mesoscale eddy scales:**
  - ➢ **WKB approximation cannot be used.**
  - ➢ **But Young and Ben Jelloul approach works!**
- **Wave-wave interactions are not neglected.**
- **Initially, waves are inertial waves with no spatial heterogeneity.**

The <u>high frequency part of the wave spectrum</u> is characterized by <u>discrete bands!</u>

<u>What mechanisms explain these characteristics?</u>

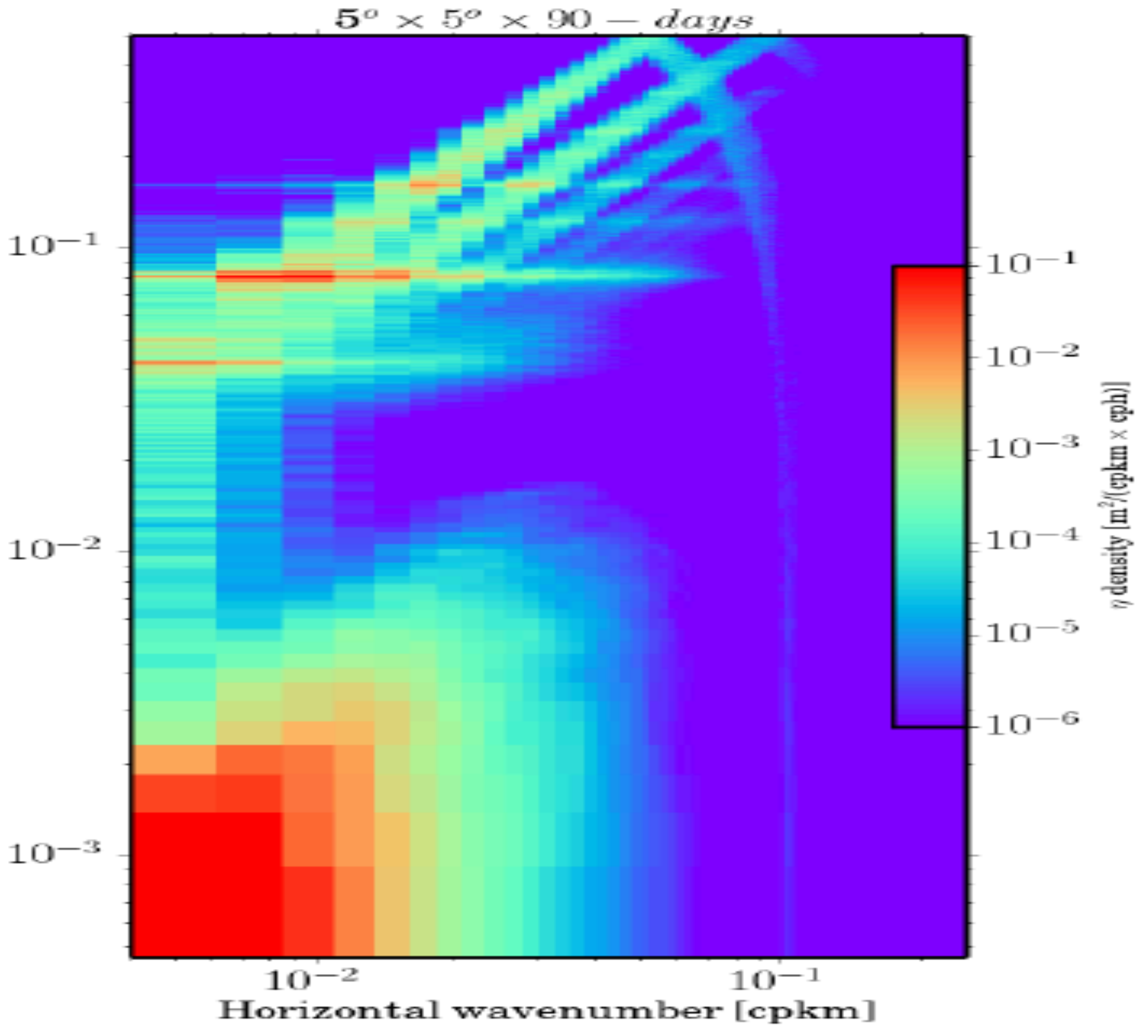

Let us consider first the dispersion of near-inertial waves by a geostrophic jet: $\boldsymbol{U(y)} = \frac{\boldsymbol{U_m}}{\boldsymbol{cosh^2\left(\frac{y}{L_m}\right)}}$ (continuous spectrum), $\boldsymbol{\zeta} = -\frac{\boldsymbol{dU}}{\boldsymbol{dy}}$.

Waves are initially homogeneous: $[\mathbf{u}, \boldsymbol{v}, \boldsymbol{h}] = [\boldsymbol{U_o}, \mathbf{0}, \mathbf{0}]$.

Equations for *u(y,t), v(y,t)* and *h(y,t)* (including nonlinear terms) are:

$$\frac{\partial u}{\partial t} + v\frac{\partial u}{\partial y} - (\mathrm{f} + \zeta)v = 0$$

$$\frac{\partial v}{\partial t} + v\frac{\partial v}{\partial y} + \mathrm{f}u = -g'\frac{\partial h}{\partial y}$$

$$\frac{\partial h}{\partial t} + \frac{\partial hv}{\partial y} + H_o\frac{\partial v}{\partial y} = 0$$

$$g' = \frac{g\Delta\rho}{\rho_o}, r^2 = \frac{g' H_o}{f^2}, \quad \frac{U_o}{fL} \approx \frac{U_m}{fL_m} \approx \varepsilon \ll 1, \quad \frac{h}{H_o} = O(\epsilon), B_u = \left(\frac{r}{L}\right)^2 = O(1), \quad \frac{L_m}{L} = O(1)$$

Wave scales can be comparable to the jet scales (continuous spectrum).

=> Young and Ben Jelloul (1998)'s approach

Nonlinear terms are not neglected but can be small.

=> Weakly nonlinear systems

$$\frac{\partial u}{\partial t} + \epsilon v \frac{\partial u}{\partial y} - (1 + \varepsilon\zeta)v = 0$$

$$\frac{\partial v}{\partial t} + \varepsilon v \frac{\partial v}{\partial y} + u = -B_u \frac{\partial h}{\partial y}$$

$$\frac{\partial h}{\partial t} + \frac{\partial(1 + \epsilon h)v}{\partial y} = 0$$

$$\frac{\partial^2 v}{\partial t^2} + (1 + \boldsymbol{\varepsilon\zeta})v - B_u \frac{\partial^2 v}{\partial y^2} = \boldsymbol{\varepsilon}\left[\boldsymbol{B_u} \frac{\boldsymbol{\partial^2 hv}}{\boldsymbol{\partial y^2}} - \frac{\boldsymbol{\partial}}{\boldsymbol{\partial t}}\left(\boldsymbol{v}\frac{\boldsymbol{\partial v}}{\boldsymbol{\partial y}}\right) + \boldsymbol{v}\frac{\boldsymbol{\partial u}}{\boldsymbol{\partial y}}\right] \quad (1)$$

We use a series expansion in ε:

$$\varphi = \varphi_o + \varepsilon\varphi_1 + \varepsilon^2\varphi_2 + O(\varepsilon^3)$$

with $\varphi = (u, v, h)$
=> Weakly nonlinear systems

$\varphi = \varphi_o + \varepsilon\varphi_1 + \varepsilon^2\varphi_2 + O(\varepsilon^3)$, with $\varphi = (u, v, h)$

At zero order we get:

$$[u_o, v_o, h] = (cost, -sint, 0)$$

From (1), equation at the first order is:

$$\frac{\partial^2 v_1}{\partial t^2} + v_1 - B_u . \frac{\partial^2 v_1}{\partial y^2} = -\boldsymbol{\zeta . v_o} \qquad (2)$$

Using: $\varphi(y, t) = \sum_k \hat{\zeta}(k, t) e^{iky}$, (2) becomes:

$$\frac{\partial^2 \widehat{v_1}(k,t)}{\partial t^2} + \widehat{v_1}(k, t)(1 + B_u . k^2) = -\boldsymbol{\hat{\zeta}(k) . v_o(\mathrm{t})} \qquad (3)$$

(scales of v_1 are comparable to ζ scales). This leads to:

$$\widehat{v_1}(k, t) = \frac{\hat{\zeta}(k)}{k^2}\left[sint - \frac{1}{\omega}\sin(\omega . t)\right]$$

with $\omega = \sqrt{1 + B_u . k^2}$

At second order eq. (1) becomes:

$$\frac{\partial^2 v_2}{\partial t^2} + v_2 - B_u . \frac{\partial^2 v_2}{\partial y^2} = \left[-\boldsymbol{v_1 . \zeta} + \boldsymbol{B_u} \frac{\boldsymbol{\partial^2 v_1 + h_1 v_o}}{\boldsymbol{\partial y^2}} - \frac{\boldsymbol{\partial}}{\boldsymbol{\partial t}} \left(\boldsymbol{v_o} \frac{\boldsymbol{\partial v_1}}{\boldsymbol{\partial y}} \right) + \boldsymbol{v_o} \frac{\boldsymbol{\partial u_1}}{\boldsymbol{\partial y}} \right] \quad (3)$$

In spectral space:

$$\frac{\partial^2 \widehat{v_2}(k,t)}{\partial t^2} + \omega^2 . \widehat{v_2}(k,t) = \boldsymbol{F(k,t)} \quad (4)$$

with $F(k,t) = -\widehat{\zeta . v_1} - B_u . k^2 v_o . \widehat{h_1} - i . k(\frac{\partial v_o . \widehat{v_1}}{\partial t} - v_o . \widehat{u_1})$

Solution for $\widehat{v_2}(k,t)$ has to be taken into account only if there is a resonance.

If we write: $\widehat{v_2}(k,t) = \sum_k \widecheck{v_2}\,(k,\Omega) e^{i\Omega t}$, and $F(k,t) = \sum_k \check{F}\,(k,\Omega) e^{i\Omega t}$,

$$(-\Omega^2 + \omega^2) . \widecheck{v_2} \; = \check{F}(k,\Omega),$$

Note that $\omega = \sqrt{1 + B_u . k^2}$. The frequencies present in (4) are: 2, $1 \pm \omega$, and $\sqrt{1 + B_u . m^2}$ (for $m \neq k$) and 1. Resonance can occur only for $\omega = 2$, which leads to $k = \sqrt{3/\sqrt{B_u}}$.

This resonance is a local phenomenon in spectral space. It can work only if $\hat{\zeta}\left(\mathrm{k} = \sqrt{3/\sqrt{B_u}}\right) \neq 0$. In dimensional variables the resonant wavelength is $l_R = \left(\frac{2\pi}{\sqrt{3}}\right) . r \approx 3.63 r$ (using $B_u = O(1)$)

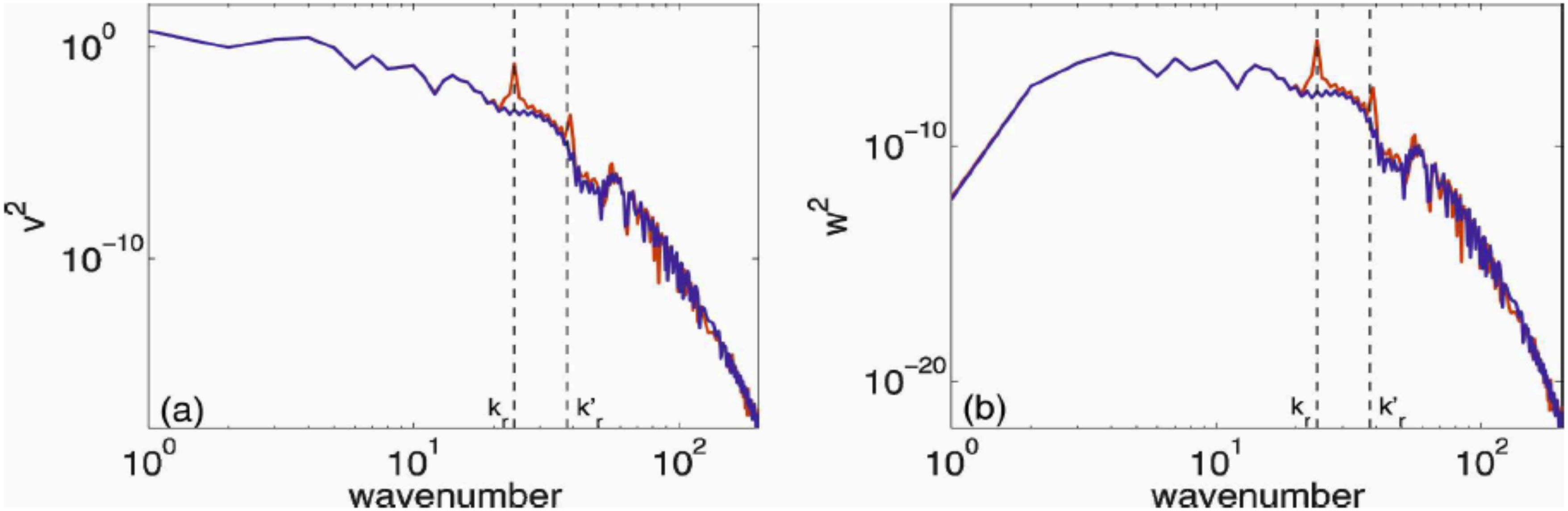

FIG. 1. Horizontal wavenumber spectra of (a) v and (b) w after eight inertial periods. Blue curves correspond to solutions of the linear system (where all the nonlinear terms have been dropped), and red curves correspond to solutions of the nonlinear system. Dashed lines represent the resonant wavenumbers $k_r = \sqrt{3}/r$ and $k'_r = \sqrt{8}/r$. The initial velocity is $u_0 = 0.3$ m s^{-1}, and the maximum jet velocity and half-width are 0.3 m s^{-1} and 20 km, respectively.

Some numerical evidence using the jet: $\boldsymbol{U(y)} = \dfrac{\boldsymbol{U_m}}{\boldsymbol{cosh^2\left(\frac{y}{L_m}\right)}}$

Resonance occurs at $\mathrm{k} = \dfrac{\sqrt{3}}{r}$, but also at $\mathrm{k} = \dfrac{\sqrt{8}}{r}$ (resonance that occurs when third order terms are taken into account).

Dispersion of internal gravity waves in a fully turbulent eddy field: Waves are forced by an homogeneous intermittent wind field

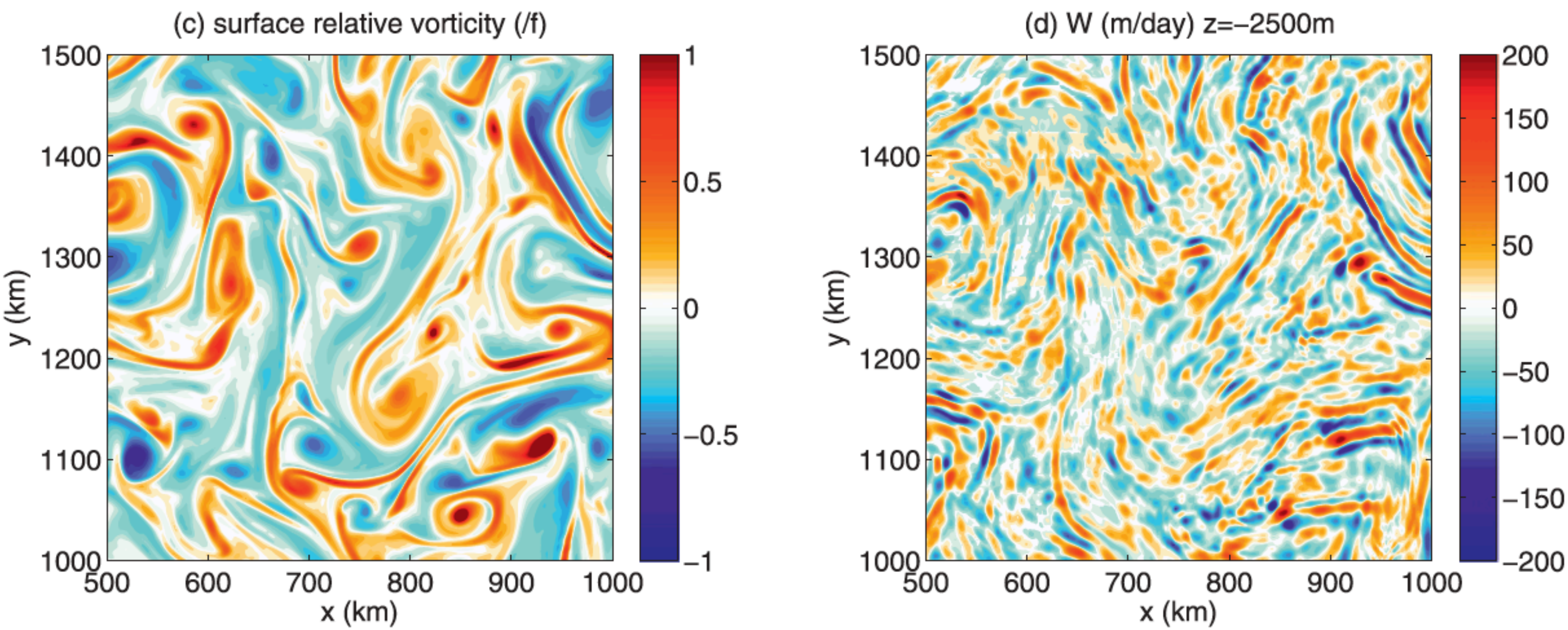

FIG. 1. Snapshots of (a),(c) the surface eddy relative vorticity field normalized by f and (b),(d) the w field (m day^{-1}) at 2500 m in the (a),(b) 6-km and (c),(d) 2-km simulations. Color scale in (a),(c) is made symmetric to equally display cyclonic and anticyclonic structures. However, relative vorticity values range between $-0.6f$ and $0.7f$ in the 6-km simulation and between $-f$ and $3f$ in the 2-km simulation.

Danioux et al. JPO 2011

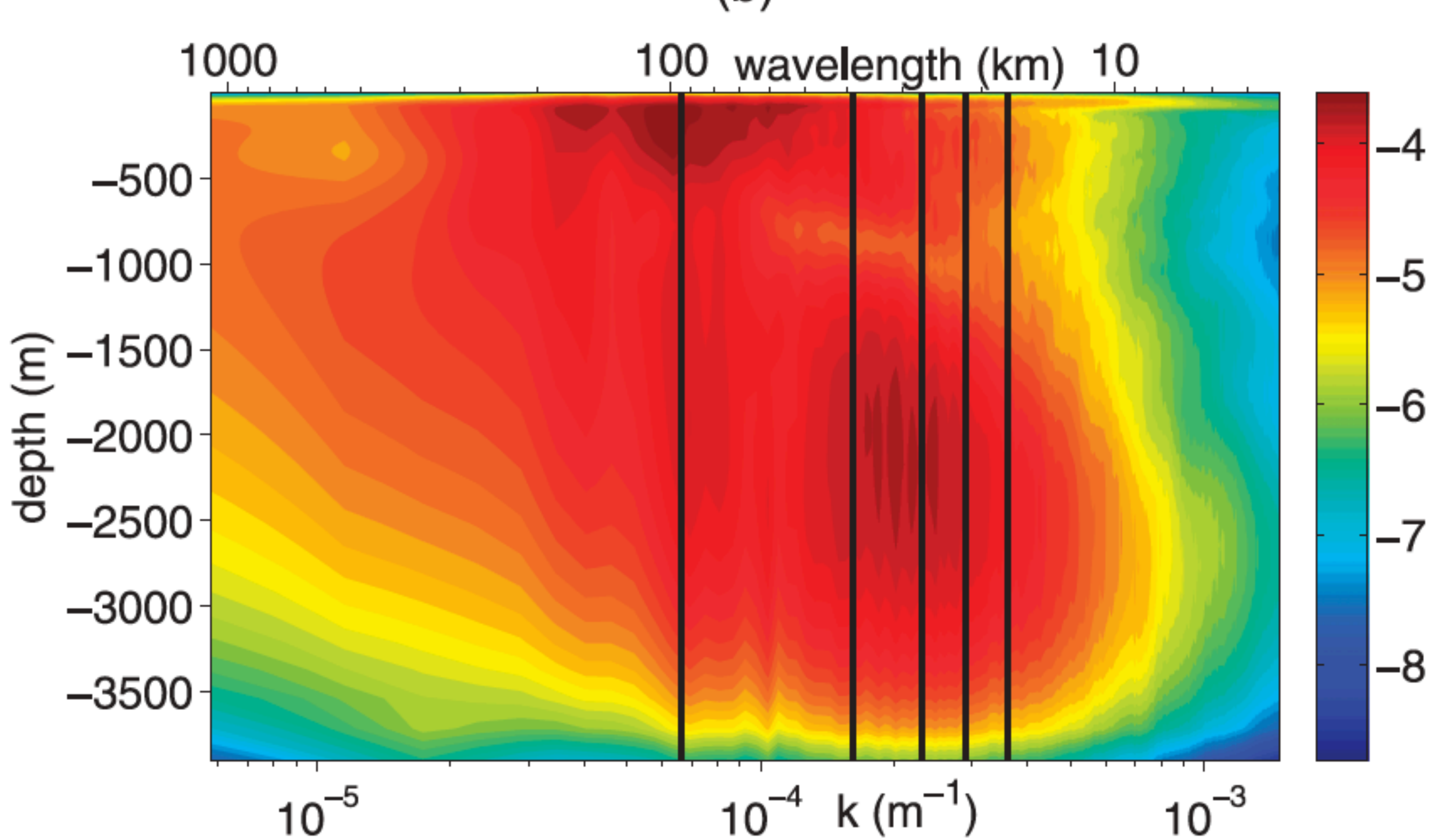

FIG. 3. (a),(b) Horizontal wavenumber spectrum of w (log scale) as a function of depth and (c),(d) frequency spectrum of w (linear scale) as a function of depth in the (a),(c) 6-km and (b),(d) 2-km simulations. The black vertical lines in Figs. 4a,b correspond to the first five resonant wavenumbers ($k_m = \sqrt{3}/r_n$, $n = 1 \ldots 5$, with r_n the Rossby radius of deformation of baroclinic mode n). They correspond to wavelengths of 92 km, 37 km, 25 km, 19 km, and 15 km, respectively.

Danioux et al. JPO 2011

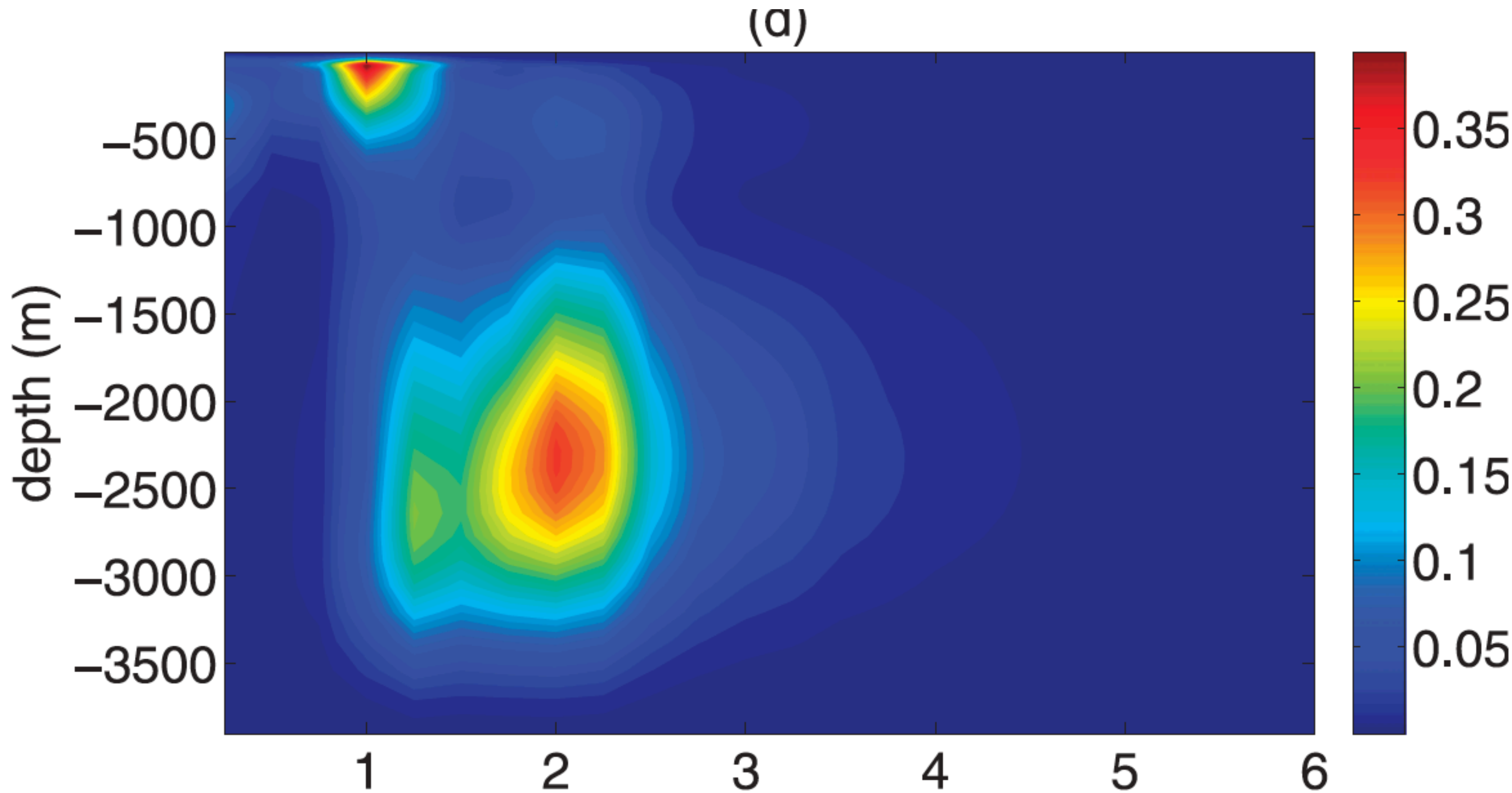

FIG. 3. (a),(b) Horizontal wavenumber spectrum of w (log scale) as a function of depth and (c),(d) frequency spectrum of w (linear scale) as a function of depth in the (a),(c) 6-km and (b),(d) 2-km simulations. The black vertical lines in Figs. 4a,b correspond to the first five resonant wavenumbers ($k_m = \sqrt{3}/r_n$, $n = 1\ldots5$, with r_n the Rossby radius of deformation of baroclinic mode n). They correspond to wavelengths of 92 km, 37 km, 25 km, 19 km, and 15 km, respectively.

Danioux et al. JPO 2011

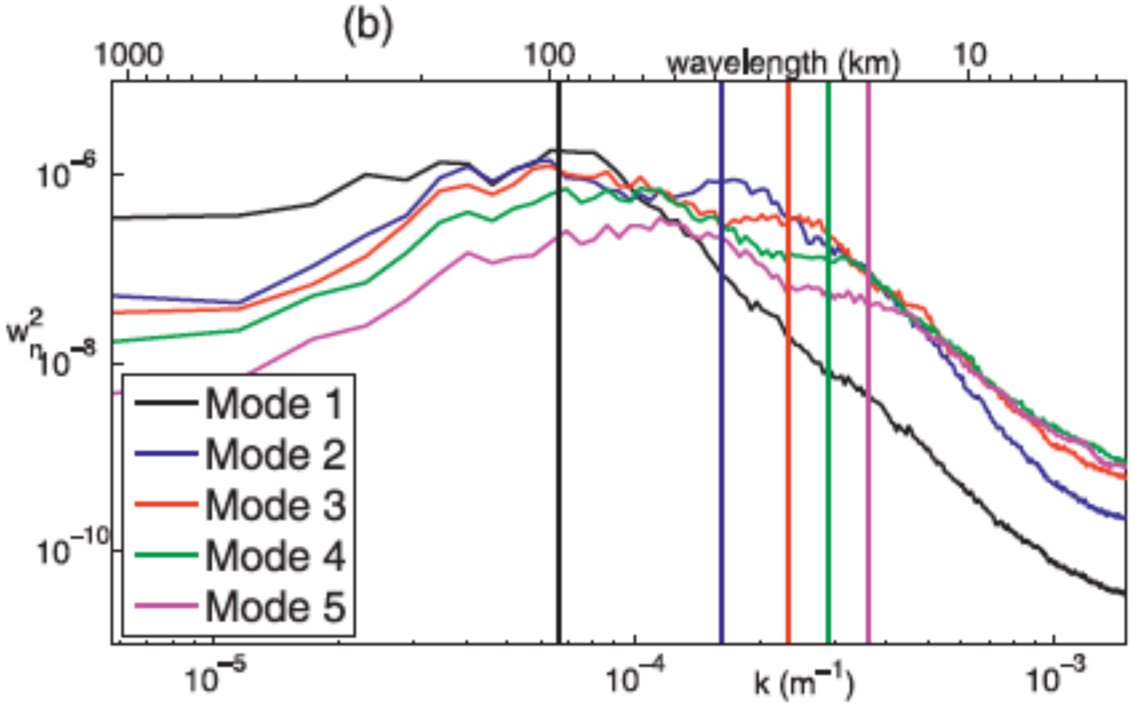

FIG. 4. Horizontal wavenumber spectrum (a),(b) of the first five modes (w_n, n = 1–5) and (c),(d) of w at 2500 m (solid curves) in the (a),(c) 6-km and (b),(d) 2-km simulations. Black vertical lines refer to the first five resonant wavenumbers k_{rn}. The dashed curves in (c),(d) correspond to the w spectrum estimated using (1) with only the first two modes.

Danioux et al. JPO 2011

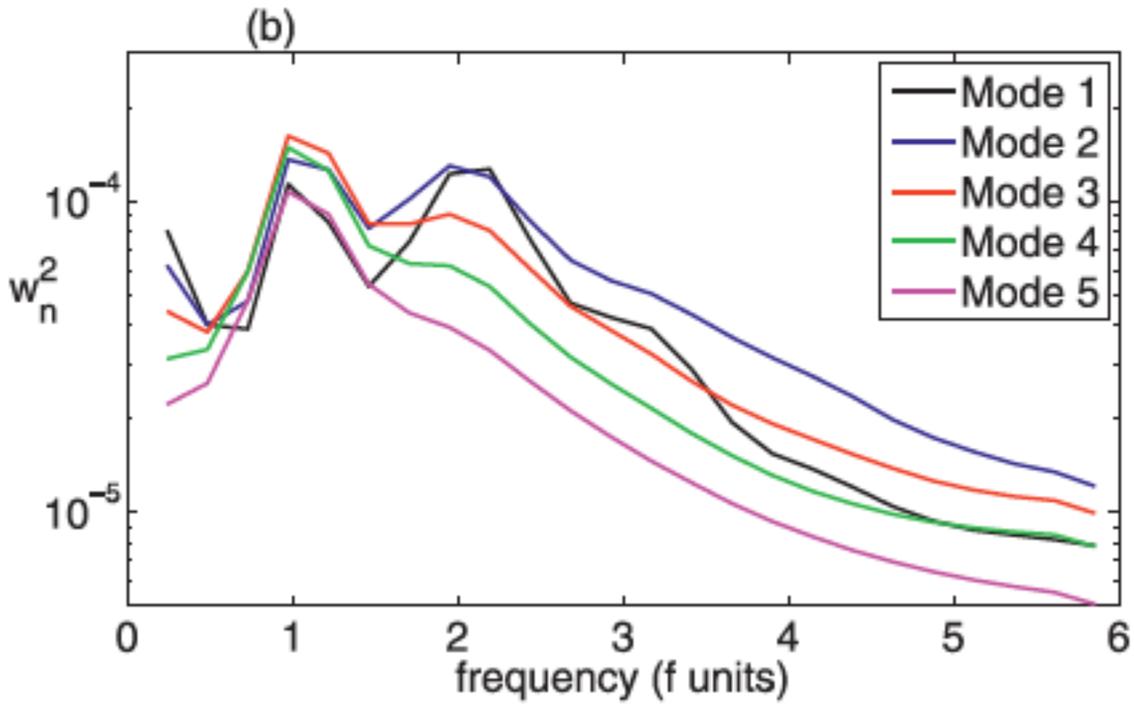

FIG. 5. Frequency spectrum (a),(b) of the first five modes (w_n, n = 1–5) and (c),(d) of w at 2500 m (solid curves) in the (a),(c) 6-km and (b),(d) 2-km simulations. The dashed curves in (c),(d) correspond to the w spectrum estimated using (1) with only the first two modes.

Danioux et al. JPO 2011

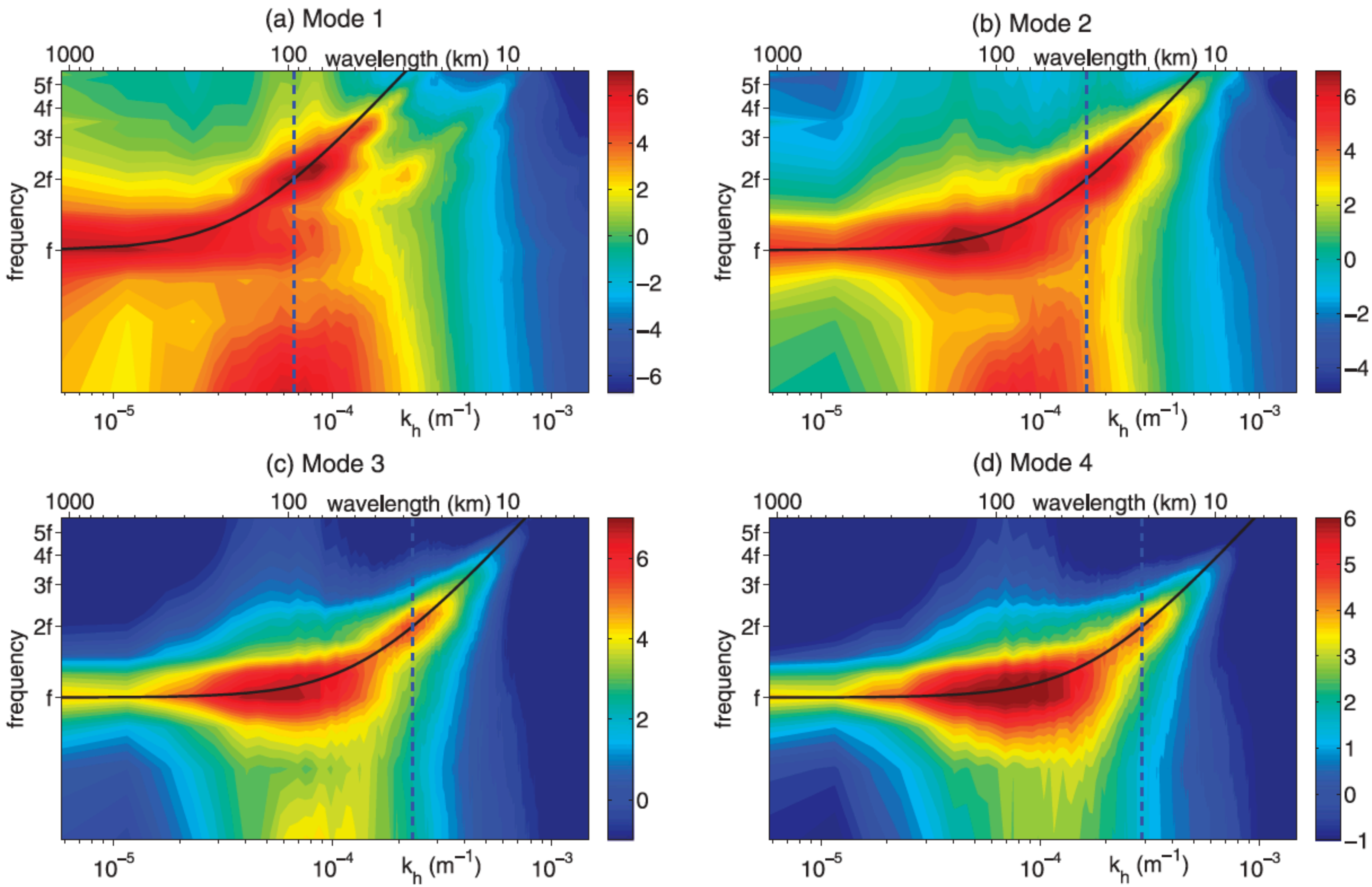

FIG. 6. Vertical kinetic energy in the frequency–wavenumber plane for the first four modes. The solid lines show the dispersion relation [$\omega_n/f = \sqrt{1 + (r_n k)^2}$, ω_n the frequency of mode n]. The dashed lines show the resonance wavenumber $k_n = \sqrt{3}/r_n$.

Danioux et al. JPO 2011

Dispersion of internal gravity waves in a fully turbulent eddy field:
Waves are forced by an homogeneous intermittent wind field

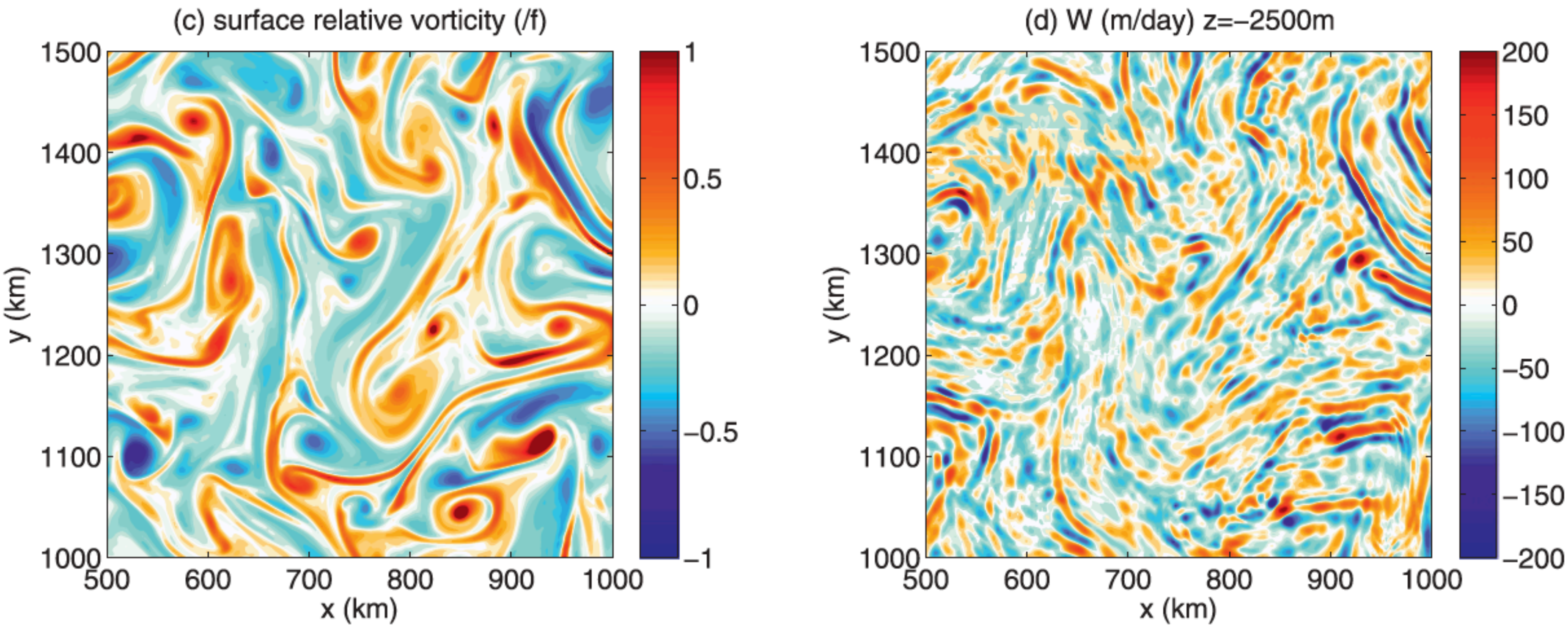

FIG. 1. Snapshots of (a),(c) the surface eddy relative vorticity field normalized by f and (b),(d) the w field (m day^{-1}) at 2500 m in the (a),(b) 6-km and (c),(d) 2-km simulations. Color scale in (a),(c) is made symmetric to equally display cyclonic and anticyclonic structures. However, relative vorticity values range between $-0.6f$ and $0.7f$ in the 6-km simulation and between $-f$ and $3f$ in the 2-km simulation.

Danioux et al. JPO 2011